

Scaling of Elliptic Flow, Recombination and Sequential Freeze-Out of Hadrons in Heavy-Ion Collisions

Min He,¹ Rainer J. Fries,^{1,2} and Ralf Rapp¹

¹*Cyclotron Institute and Department of Physics and Astronomy,
Texas A&M University, College Station, TX 77843, USA*

²*RIKEN/BNL Research Center, Brookhaven National Laboratory, Upton, NY 11973, USA*

(Dated: November 2, 2021)

The scaling properties of elliptic flow of hadrons produced in ultrarelativistic heavy-ion collisions are investigated at low transverse momenta, $p_T \lesssim 2$ GeV. Utilizing empirical parameterizations of a thermalized fireball with collective-flow fields, Resonance Recombination Model (RRM) is employed to describe hadronization via quark coalescence at the hadronization transition. We reconfirm that RRM converts equilibrium quark distribution functions into equilibrated hadron spectra including the effects of space-momentum correlations on elliptic flow. This provides the basis for a controlled extraction of quark distributions of the bulk matter at hadronization from spectra of multi-strange hadrons which are believed to decouple close to the critical temperature. The resulting elliptic flow from empirical fits at RHIC exhibits transverse kinetic-energy and valence-quark scaling. Utilizing the well-established concept of sequential freeze-out we find that the scaling at low momenta can be extended to bulk hadrons (π , K , p) at thermal freeze-out, and thus result in an overall description compatible with both equilibrium hydrodynamics and quark recombination.

PACS numbers: 25.75.-q, 12.38.Mh, 14.40.Lb

Keywords: Resonance Recombination, Sequential Freeze-out, KE_T -scaling

I. INTRODUCTION

Ultrarelativistic heavy-ion collisions (URHICs) enable the creation and study of superdense strongly interacting matter, possibly associated with the formation of novel phases where partons deconfine and chiral symmetry is restored [1]. One major finding by the experimental program at the Relativistic Heavy Ion Collider (RHIC) at Brookhaven National Laboratory is the large azimuthal anisotropy of hadron transverse-momentum (p_T) spectra in non-central nuclear collisions, the so-called elliptic flow [2]. It is quantified by the second harmonic coefficient, $v_2(p_T)$, in the Fourier expansion of the azimuthal angle, ϕ , for the p_T -spectra of hadrons.

Experimental measurements suggest that the behavior of $v_2(p_T)$ may be classified into three regimes. At high transverse momentum, $p_T \gtrsim 6$ GeV, the azimuthal anisotropy is believed to be due to the path-length dependence of high-energy partons as they traverse the hot medium and lose energy. We will not be concerned any further with this mechanism in the present work. At low transverse momentum, $p_T \lesssim 2$ GeV, v_2 increases with p_T essentially linearly but with a delayed onset for hadrons with increasing mass, giving rise to the so-called mass ordering of elliptic flow [3]. This regime is well described by hydrodynamic simulations and thus indicates a large degree of equilibration, encompassing more than 90% of the observed particles [4–8]. At intermediate transverse momenta, $2 \text{ GeV} \lesssim p_T \lesssim 6 \text{ GeV}$, $v_2(p_T)$ saturates and exhibits a remarkable scaling between baryons and mesons [9],

$$v_2(p_T) = n_q v_2^{(q)}(p_T/n_q), \quad (1)$$

where n_q denotes the number of valence quarks contained

in hadron h . Equation (1), also known as “constituent-quark number scaling” (CQNS), has been successfully described in the framework of quark coalescence models, where quarks recombine into hadrons at the transition from partonic to hadronic matter [10]. In line with Eq. (1), these models thus imply that the observed hadron elliptic flow can be reduced to a universal quark elliptic flow at hadronization. This assertion, however, requires several simplifying assumptions. First, interactions in the subsequent hadronic evolution (between hadronization at $T_c \simeq 170$ MeV and kinetic freeze-out at $T_{fo} \simeq 110$ MeV) are neglected. Furthermore, Eq. (1) can only be derived in instantaneous quark coalescence models where energy conservation is violated and narrow hadron wave functions in momentum space are utilized. In addition, the underlying quark distribution functions are assumed to factorize in coordinate and momentum space, implying that the elliptic flow of the system is implemented point-by-point (i.e., locally), rather than through a space-dependent flow field which is a consequence of a collectively expanding source. The implementation of realistic space-momentum correlations into quark coalescence models has indeed been proved difficult [11]. Finally, quark coalescence models typically do not comply with the principle of detailed balance, implying that the proper equilibrium limit cannot be established. This hampers attempts to extend the description into the low- p_T regime where thermalization is believed to prevail. This has become a more pressing issue once it was realized that CQNS can be generalized to encompass both low and intermediate p_T if v_2 is plotted versus transverse kinetic energy, $KE_T \equiv m_T - m$, where $m_T = (p_T^2 + m^2)^{1/2}$ is the hadron’s transverse mass [12–17]. In this representation, elliptic-flow data for all ob-

served hadrons fall onto one universal curve for v_2/n_q versus KE_T/n_q [12, 13].

Progress on the above issues has been recently reported by reformulating the quark-coalescence process at hadronization in terms of resonant $q\bar{q} \rightarrow M$ scattering (M : meson) [18, 19]. Implementing the underlying cross section into a Boltzmann transport equation (e.g., in Breit-Wigner approximation) not only guarantees energy-momentum conservation but also satisfies detailed balance and thus leads to the correct thermal-equilibrium limit. It has been verified [18] that the meson spectra resulting from the Resonance Recombination Model (RRM) are compatible with CQNS, Eq. (1), in the factorized (local) approximation to $v_2(p_T)$. A further step has been taken in Ref. [20] where the RRM has been applied to more realistic quark distribution functions as generated by relativistic Langevin simulations within an expanding QGP fireball [21] for semi-central Au-Au collisions at RHIC. Since the Brownian-motion approximation underlying the Langevin process is only reliable for relatively massive and/or high-momentum particles, $m_T \gg T$, the results have been restricted to charm and strange quarks. Under inclusion of the full space-momentum correlations imprinted on the quark distributions by the hydro-like flow fields of the expanding fireball, the elliptic flow of ϕ and J/ψ mesons was found to exhibit CQNS in KE_T from 0 to ~ 3 GeV, which encompasses both low and intermediate p_T , i.e., the quasi-thermal and kinetic regimes. However, several important questions remain, e.g., the manifestation of CQNS and KE_T scaling for bulk (light) particles in the low- p_T (thermal) regime, the robustness and generality of the flow fields utilized in the fireball simulations or the role of reinteractions in the hadronic phase. A thorough understanding of these issues, in connection with a quantitative description of hadron data, is hoped to ultimately enable the extraction of quark distribution functions just prior to the conversion to hadronic degrees of freedom, and thus to quantitatively establish the presence of a collectively expanding partonic source in URHICs.

In the present paper we conduct investigations of scaling properties of hadron spectra by focusing on the low- p_T regime coupled with the assumption of complete kinetic equilibration. We will utilize the RRM to convert locally equilibrated quark distribution functions into hadron spectra using a blast-wave type quark source with realistic flow fields at the hadronization transition (including space-momentum correlations characteristic of hydrodynamic simulations). Contrary to earlier work [20], we do not attempt to generate the flow fields from a dynamic evolution, but rather extract them from empirical fits to hadron p_T -spectra and elliptic flow. In fact, after verifying that resonance recombination converts collective, locally equilibrated quark distribution functions into equilibrium hadron distributions with identical (space-momentum dependent) collective properties, one can adopt the source parametrization at the hadron level and thus readily extend the description

to baryons. For this part of the investigation we focus on multi-strange hadrons (i.e., hadrons containing at least 2 strange and/or anti-strange quarks) which are believed to kinetically decouple close to the hadronization transition. This notion is supported by empirical blast-wave fits to RHIC and SPS data [1, 22, 23], as well as by the putative absence of resonances that these hadrons could form in interactions with bulk particles such as pions, kaons or nucleons (hadronic resonances drive the collective expansion of the hadronic phases in URHICs). We refer to hadrons decoupling close to T_c as “group-I” particles, which are thus the prime candidates to infer properties of the quark phase just above the critical temperature. On the other hand, the most prominent bulk particles (π , K , p , etc.) are well-known to interact quasi-elastically via strong hadronic resonances, such as $\rho(770)$, $K^*(892)$ and $\Delta(1232)$, which renders their interactions operative until a kinetic freeze-out temperature, T_{fo} , which is significantly lower than the one of group-I particles, $T_{fo} \simeq 110$ MeV $<$ $T_c \simeq 170$ MeV. We refer to hadrons decoupling at T_{fo} as “group-II” particles. Clearly, a description of KE_T scaling in the low- p_T regime would be incomplete (to say the least) without π , K and p . In an attempt to include these particles, we adopt the simplest possible scenario of introducing a second source for group-II particles by fitting their spectra and v_2 with a space-dependent elliptic flow field at T_{fo} . We then evaluate in how far such a minimalistic (but in our opinion well-motivated) sequential freeze-out can be compatible with CQNS and KE_T scaling, and which mechanisms could be responsible for them. In doing so we also revisit the question of resonance feed-down contributions to the pion v_2 for which differing results seem to exist in previous works.

Our article is organized as follows. In Sec. II we recapitulate basic features of the RRM, specifically its equilibrium limit in the presence of anisotropic flow fields. In Sec. III we quantitatively construct realistic flow fields for semi-central Au-Au collisions at RHIC using group-I particle freeze-out close to the hadronization transition. In Sec. IV we reiterate this procedure for group-II particles at kinetic freeze-out. In Sec. V we examine our results for group-I and -II particles with respect to CQNS and KE_T scaling. The effects of feed-down on the inclusive pion v_2 are revisited in App. A. We summarize and conclude in Sec. VI.

II. RESONANCE RECOMBINATION MODEL AND EQUILIBRIUM LIMIT

Early quark coalescence models which employed instantaneous approximations in the recombination of quarks [10, 24] were quite successful in providing an explanation for two rather unexpected phenomena in hadron spectra at intermediate p_T in Au-Au collisions

at RHIC.¹ Specifically, these were the enhancement of baryon-to-meson ratios ($B/M = p/\pi, \Lambda/K$) over their values measured in p - p collisions, as well as CQNS of $v_2(p_T)$. While an enhanced B/M ratio is also a natural outcome of hydrodynamic flow, the latter is not expected to generate enough yield to dominate hadron production at $p_T > 2 - 3$ GeV. The instantaneous projection of parton states onto hadron states conserves 3-momentum by construction but energy conservation is violated due to the sudden approximation [11]. This approximation is believed to be viable at intermediate p_T where corrections are expected to be of order $\mathcal{O}(Q/p_T)$ with $Q = m - m_q - m_{\bar{q}}$ (m : meson mass, $m_{\bar{q},q}$: anti-/quark mass), albeit with unknown coefficient [18]. However, this poses a significant problem at low p_T and/or for hadrons (resonances) with large binding energy (Q -value).

In Ref. [18] quark coalescence in an interacting medium in the vicinity of the hadronization transition was reinterpreted as a process akin to the formation of resonances, $q + \bar{q} \rightleftharpoons M$, and implemented via a Boltzmann equation

$$p^\mu \partial_\mu f_M(t, \vec{x}, \vec{p}) = -m\Gamma f_M(t, \vec{x}, \vec{p}) + p^0 \beta(\vec{x}, \vec{p}), \quad (2)$$

where $f_M(t, \vec{x}, \vec{p})$ denotes the phase space density of the meson, and the gain term is given by

$$\begin{aligned} \beta(\vec{x}, \vec{p}) &= \int \frac{d^3 p_1 d^3 p_2}{(2\pi)^6} f_q(\vec{x}, \vec{p}_1) f_{\bar{q}}(\vec{x}, \vec{p}_2) \\ &\times \sigma(s) v_{\text{rel}}(\vec{p}_1, \vec{p}_2) \delta^3(\vec{p} - \vec{p}_1 - \vec{p}_2). \end{aligned} \quad (3)$$

The use of an explicit (resonant) cross section automatically satisfies energy-momentum conservation. For simplicity it has been modeled by a relativistic Breit-Wigner form,

$$\sigma(s) = g_\sigma \frac{4\pi}{k^2} \frac{(\Gamma m)^2}{(s - m^2) + (\Gamma m)^2}, \quad (4)$$

where the same reaction rate Γ is used as in the loss term, the first term on the right-hand-side (*rhs*) of Eq. (2), and g_σ is the degeneracy factor. This guarantees detailed balance, which is essential for recovering thermodynamic equilibrium in the long-time limit, $\Delta\tau \gg 1/\Gamma$. If hadronization is rapid enough to produce hadrons in equilibrium, as it seems to be the case for the bulk of hadrons in URHICs, this limit is applicable and the resulting hadron-momentum distribution is given by

$$f_M^{eq}(\vec{p}) = \frac{E_M(\vec{p})}{m\Gamma} \int d^3 x \beta(\vec{x}, \vec{p}) \quad (5)$$

For more details, we refer the reader to Ref. [18]. It is well known that the unique equilibrium solution of a

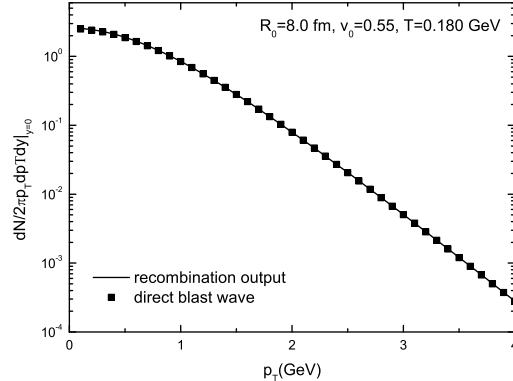


FIG. 1: (Color online) Comparison of ϕ -meson p_T spectra computed from (i) resonance recombination of strange quarks using blast-wave flow fields for strange quarks (rectangles), and (ii) a direct application of an equilibrium blast-wave distribution (solid line) with the same flow field as for quarks (solid line). The hadronization temperature has been chosen at $T_c = 180$ MeV and the radial flow at the surface as $v_0 = 0.55$.

Boltzmann transport equation is a Boltzmann distribution if and only if energy conservation as well as detailed balance are satisfied. The RRM complies with these requirements. In the remainder of this section we will verify numerically that Eq. (5) recovers the thermal Boltzmann distribution for mesons in the presence of a spatially dependent anisotropic flow field at the quark level (in previous work [18, 20], this has only been exemplified for p_T spectra, not for v_2).

As a first test we study ϕ mesons in an azimuthally symmetric and longitudinally boost-invariant fireball. The phase space-densities of the input strange and anti-strange quarks ($m_s = 0.45$ GeV) are parameterized through a blast-wave with radial flow velocity $\vec{v}(\vec{r}) = v_0 \cdot \vec{r}/R_0$. We compare the result for ϕ mesons ($m_\phi = 1.02$ GeV, $\Gamma_\phi = 0.05$ GeV) calculated from resonance recombination of s and \bar{s} , Eq. (5), with the direct blast-wave expression for the ϕ meson with identical flow field and temperature as for the quark input. Fig. 1 shows that both ways of computing the ϕ spectra are in excellent agreement. We have reconfirmed that the results are insensitive to variations of the resonance width Γ when ensuring $\Gamma \lesssim Q$ with $Q = m_\phi - (m_s + m_{\bar{s}})$ [18].

To account for anisotropic flow fields which are suitable for generating configurations reminiscent of hydrodynamic simulations for fireballs in non-central (azimuthally asymmetric) nuclear collisions, we adopt in this work the parameterization introduced by Retière and Lisa (RL) [25]. It assumes longitudinal boost-invariance [26] and parameterizes the transverse flow rapidity as a function of radius r and spatial azimuthal

¹ Throughout this manuscript, we will use p_T (p_t) to denote hadron (quark) transverse momenta.

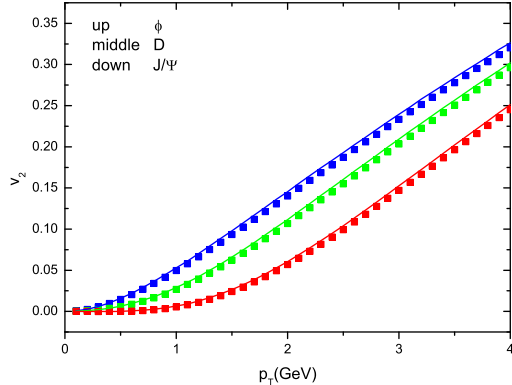


FIG. 2: (Color online) Comparison of elliptic flow for ϕ , D and J/ψ mesons (top to bottom) computed from: (i) resonance recombination of strange quarks (symbols), and (ii) a direct application of the blast-wave expression at the meson level (lines). Both quark and meson distributions are based on the same anisotropic flow field constructed from the RL parameterization with $T_c = 180$ MeV, $R_x = 7.5$ fm, $R_y = 8.5$ fm, $\rho_0 = 0.66$ and $\rho_2 = 0.07$.

angle ϕ_s as

$$\rho(r, \phi_s) = \tilde{r}[\rho_0 + \rho_2 \cos(2\phi_b)] , \quad (6)$$

where ρ_0 represents the average radial flow rapidity and ρ_2 the anisotropy of transverse flow. The angle ϕ_b of the flow vector is generally tilted from the position angle ϕ_s (both angles are measured with respect to the reaction plane) which can be reflected by the relation

$$\tan \phi_b = \left(\frac{R_x}{R_y} \right)^2 \tan \phi_s . \quad (7)$$

This ansatz is motivated by the picture that the transverse boost is locally perpendicular to elliptical subshells [25]. The transverse flow rapidity, $\rho(r, \phi_s)$, is assumed to increase linearly with the normalized "elliptic radius", defined as

$$\tilde{r} = \sqrt{r^2 \cos^2 \phi_s / R_x^2 + r^2 \sin^2 \phi_s / R_y^2} . \quad (8)$$

We emphasize that this flow field incorporates space-momentum correlations that are considered a much more realistic representation of a collectively expanding source than the factorized ansatz of a "local" v_2 (independent of position) as often adopted in quark coalescence models calculations.

Using the RL parameterization the differential momentum spectrum for a particle i directly emitted from the source takes the form [5, 25, 27] (feed-down contributions are evaluated in App. A)

$$\frac{dN_i}{p_T dp_T d\phi_p dy} = \frac{2g_i}{(2\pi)^3} \tau_f m_T e^{\mu_i/T_f} \times \int r dr \int d\phi_s K_1(m_T, T, \beta_T) e^{\alpha_T \cos(\phi_p - \phi_b)} , \quad (9)$$

where T_f is the freeze-out temperature at constant longitudinal proper time τ_f , μ_i the chemical potential of particle i , g_i the spin-isospin degeneracy factor, K_1 a modified Bessel function and $\alpha_T = p_T/T_f \sinh \rho(r, \phi_s)$, $\beta_T = m_T/T_f \cosh \rho(r, \phi_s)$. Equation (9) has been written in Boltzmann approximation which works well for sufficiently heavy particles; we will, however, use Bose distributions for pions. From Eq. (9) we can calculate the elliptic flow of particle i as

$$v_2^i(p_T) = \frac{\int_0^{2\pi} d\phi_p \cos(2\phi_p) \frac{dN_i}{p_T dp_T d\phi_p dy}}{\int_0^{2\pi} d\phi_p \frac{dN_i}{p_T dp_T d\phi_p dy}} . \quad (10)$$

With the RL parameterization for an anisotropic flow field we are now in position to compare the elliptic flow generated for coalesced mesons in the RRM for locally equilibrated quark distributions, Eq. (5) with the one directly obtained from applying the blast-wave expression (9) at the meson level. We fix the parameters as quoted in the caption of Fig. 2, noting that at this point our aim is not to fit experimental data but to scrutinize generic properties of the RRM. We emphasize again the nontrivial spatial dependence of the flow field figuring into the quark distributions in Eq. (5). To extend the scope of our comparison we consider, in addition to ϕ mesons, also D ($m_D = 1.9$ GeV, $\Gamma_D = 0.1$ GeV) and J/ψ mesons ($m_{J/\psi} = 3.1$ GeV, $\Gamma_{J/\psi} = 0.1$ GeV), as bound states of charm ($m_c = 1.5$ GeV) and light quarks ($m_{u,d} = 0.3$, GeV) and of charm and anticharm quarks, respectively. Fig. 2 illustrates the comparison of the meson- $v_2(p_T)$ for RRM and their direct blast-wave counterparts, showing again excellent agreement within numerical accuracy. It is quite remarkable that RRM generates negative v_2 at low p_T for the J/ψ starting from strictly positive $v_2(p_t)$ for the underlying charm-quark distributions. A possibly negative v_2 is a well-known mass effect caused by the depletion of the heavy-particle yield at low momenta in the presence of sufficiently large collective flow [7]. However, we are not aware of any quark coalescence model calculation that has reproduced this result. It demonstrates that the meson distributions resulting from RRM have reached local equilibrium and follow the collective flow of the source. We have checked that the negative v_2 is rather robust against variations of blast-wave parameters. By increasing ρ_0 or ρ_2 the negative value can be amplified.

Combining the results from Figs. 1 and 2, we conclude that hadron phase-space distributions obtained from resonance recombination precisely reflect the collective properties of a source in local equilibrium, explicitly documenting the fact that the RRM achieves this through energy conservation and detailed balance. These insights also imply that the intermediate- p_T regime, where v_2 saturates and shows an explicit dependence on quark number, can not be in full equilibrium.

Group	T_f	ρ_0	ρ_2	R_x	R_y
I	180	0.75	0.072	7.5	8.9
II	110	0.93	0.055	11.0	12.4

TABLE I: Parameter values for kinetic freeze-out temperature, T_f in MeV, radial-flow rapidity ρ_0 , rapidity-asymmetry, ρ_2 , and elliptic radii, R_x and R_y in fm, for group-I and -II hadrons using the RL blast-wave expression for mid-central Au-Au collisions at RHIC.

III. RECOMBINATION AND QUARK DISTRIBUTIONS AT HADRONIZATION

Based on the verification that resonance recombination maps the collective local-equilibrium properties of the quark source into hadron spectra, we can reverse the strategy and use this as a tool to extract quark distributions by a quantitative study of experimental data on hadrons which arise from quark coalescence. The generality of this argument even allows to extend the analysis to baryons without having to explicitly calculate their spectra in RRM (which would be more involved than for mesons as it requires to recombine 3 quarks). As alluded to in the introduction, this procedure can only give access to quark distributions if the subsequent hadronic phase exerts a negligible distortion of the hadron spectra right after their formation around T_c . We label such hadrons as belonging to “group I”, and identify multi-strange hadrons (ϕ , Ξ , Ω) as the prime candidates currently available from experiment. These hadrons have no well-established resonance excitations on the most abundant bulk particles (π , K and N) in the hadronic medium, while elastic t -channel exchange processes are suppressed by the OZI rule. One can therefore expect that multi-strange hadrons do not suffer significant rescattering in the hadronic phase, which is indeed supported by blast-wave fits to experimental data favoring kinetic decoupling not far from T_c . The flow fields extracted for group-I hadrons therefore reflect the collective properties of the quark phase.

We first determine the flow parameters in the RL parameterization by performing a blast-wave fit to the transverse-momentum spectra and elliptic flow of group-I hadrons to experimental data from STAR in mid-central (20-40%) Au-Au collisions. For definiteness (and easier comparison to the RRM calculations in Ref. [20]), we fix the temperature to $T_c = 180$ MeV; we do not utilize it as a parameter but obtain fits of satisfactory quality with this value. The transverse-flow rapidity, ρ_0 , is mostly governed by fits to the p_T -spectra of ϕ , Ξ and Ω hadrons, while the flow-asymmetry parameter, ρ_2 , and the fireball’s spatial eccentricity, R_y/R_x , are driven by fitting the elliptic flow of Ξ and ϕ . The resulting RL blast-wave curves are shown with data in Fig. 3, and the central values of the parameters are collected in Tab. I. As to be expected, the slopes of the spectra can be fitted well. The absolute normalizations are also repro-

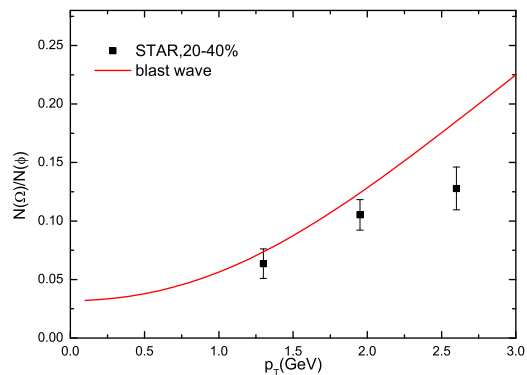
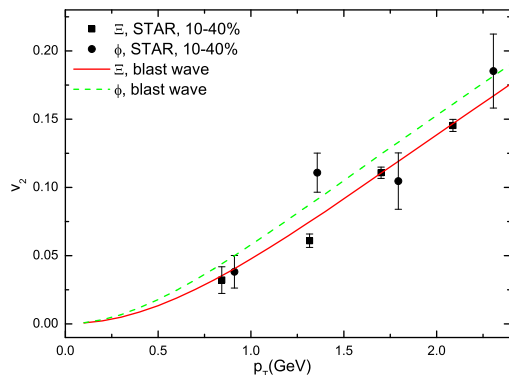
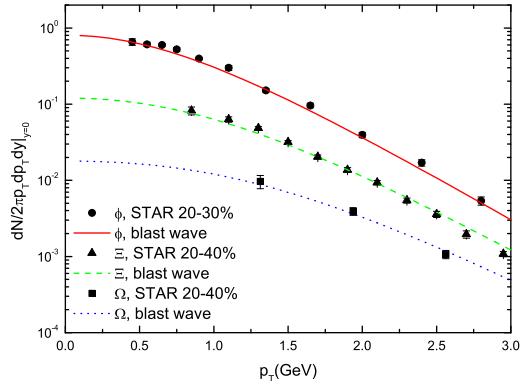


FIG. 3: (Color online) Blast-wave fits to STAR data [13, 29–31] in semi-central Au-Au ($\sqrt{s_{NN}}=200$ GeV) collisions for transverse-momentum spectra (upper panel) and elliptic flow (middle panel) of ϕ , Ξ^+ and $(\Omega + \bar{\Omega})/2$ using the RL ansatz with parameters specified in Tab. I. The lower panel shows the resulting Ω -to- ϕ ratio on a linear scale, compared to STAR data [29].

duced reasonably as well, which is confirmed by the Ω -to- ϕ ratio shown on a linear scale in the lower panel of Fig. 3. Degeneracy factors for spin and isospin are taken into account, but baryon chemical potential and

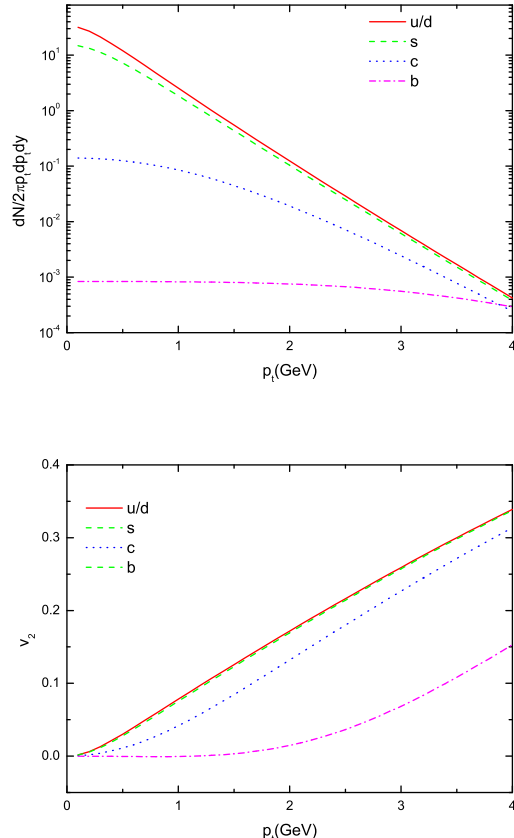


FIG. 4: (Color online) Upper panel: Equilibrated transverse momentum distributions of quarks on a hypersurface with temperature just above T_c for a mid-central fireball at RHIC energies as predicted by the RRM model from group I data. Bottom panel: The same for the v_2 of the equilibrated quarks.

the strangeness suppression factor, γ_s , are neglected in these fits (they contribute at the 10% level which can easily be absorbed by fine-tuning the freeze-out temperature). Note that the Ω -to- ϕ ratio is quite different from linear for p_T up to ~ 1.5 GeV, and that this ratio does not go to zero for $p_T \rightarrow 0$ as predicted by quark coalescence models discussed in Ref. [28, 29]. This reiterates once more the importance of energy conservation and the thermal-equilibrium limit if one attempts to describe hadron spectra through quark coalescence in the low- p_T regime.

We are now in a position to extract the quark distribution functions at hadronization by assuming that: (i) the flow field for group-I hadrons is indeed the flow field for the hadronic phase in equilibrium just below T_c (which is further supported by the fact that it is possible to use a freeze-out temperature of 180 MeV), and (ii) group-I hadron formation occurs via coalescence from a partonic phase (which is supported by the general CQNS characteristics of RHIC data). In Fig. 4 we not only include the

extracted strange- and light-quark spectra and elliptic flow (which are directly involved in the RRM-based fits) but also those implied for the heavier charm and bottom quarks. Equilibration of the latter 2 quark flavors is currently an open issue, but this may rather be a question of how far up in p_t it applies. Qualitatively, the same limitation applies to light and strange quarks, which presumably enter the kinetic regime at $p_t \simeq 1$ GeV, where the data for the quark-number scaled v_2 level off at a value of about 7-8%. Once available, D - and B -meson data will allow for similar estimates, and we provide here the underlying heavy-quark spectra as a reference for such an analysis.

An extraction of strange- and light-quark spectra in a similar spirit, i.e., from data of what we refer to as group-I hadrons, has been attempted by in Ref. [32] based on a 1-dimensional instantaneous quark coalescence model. We reiterate here that such an extraction cannot be reliably applied at low p_T due to the simplifying assumptions inherent to such models, but it would certainly be interesting to make a comparison between both approaches.

IV. SEQUENTIAL FREEZE-OUT AND BULK PARTICLES

In URHICs the most abundant bulk particles, like pions, kaons and protons (which we refer to as group-II particles), undergo significant re-scattering in the hadronic phase. This is borne out of experimental blast-wave fits which require kinetic-freeze-out temperatures (e.g., $T_{fo} \simeq 100$ MeV for central Au-Au collisions at RHIC [1]) which are significantly lower than the chemical freeze-out temperatures ($T_{ch} \simeq 160 - 180$ MeV, extracted from observed ratios of different hadron species). Note that the difference in the kinetic and chemical freeze-out temperatures translates into a factor 5-10 different energy densities [33]. Theoretically, the sequential freeze-out systematics can be readily understood from large resonant cross sections operative for group-II particles in the hadronic phase, e.g., $\pi\pi \rightarrow \rho \rightarrow \pi\pi$, $\pi K \rightarrow K^* \rightarrow \pi K$ or $\pi N \rightarrow \Delta \rightarrow \pi N$. The values of these elastic cross sections reach up to 100-200 mb and are thus 1-2 orders of magnitude larger than chemistry-changing inelastic ones (e.g., $\pi\pi \rightarrow KK$). Further direct evidence for an extended duration of hadronic reinteractions follows from the well-established low-mass dilepton enhancement in URHICs whose magnitude and spectral shape requires several generations of ρ mesons to form with a largely broadened spectral shape due to a strong coupling to the medium [34].

In order to include group-II particles in an analysis of the thermal regime of anisotropic flow fields there is thus no choice but to introduce an additional source parameterization at a much lower temperature than for group-I particles. While this generally detaches group-II particles from coalescence mechanisms at hadronization, we remark that their production through resonance recom-

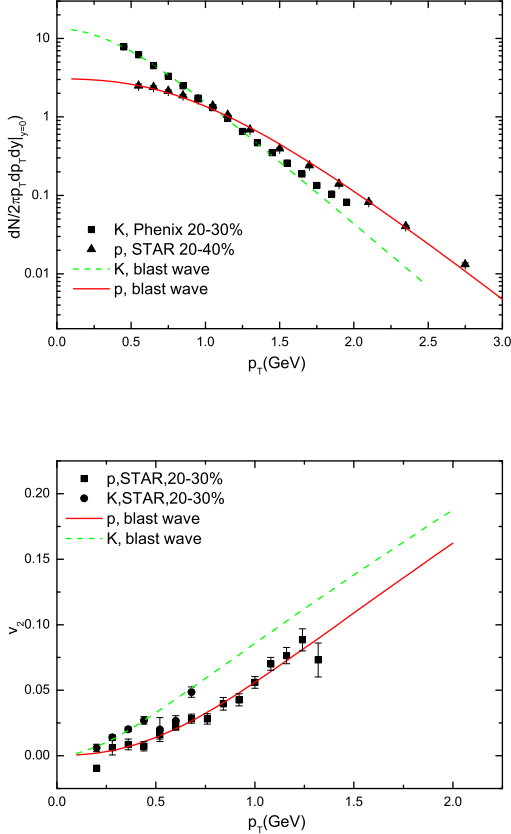


FIG. 5: (Color online) Blast-wave fits using the RL fireball parameterization to proton and kaon p_T -spectra (upper panel) and elliptic flow (lower panel) in mid-central Au-Au collisions at RHIC. The flow-field source parameters are listed in Tab. I. Experimental data are taken from Refs. [3, 35, 36].

bination in equilibrium at T_c by no means contradicts but rather facilitates local equilibrium until a much lower bulk freeze-out. Group-II hadrons at low p_T are therefore not suitable to infer direct statements about quark recombination. Our aim rather is to test whether the minimal assumption of a sequential freeze-out is sufficient to produce the general scaling properties observed in the data, and, if so, what the key features are and how sensitive this picture is to variations of the freeze-out configuration. We note in passing that the situation is presumably quite different at intermediate p_T where hadronic re-scattering is insufficient to maintain equilibrium and one is rather dealing with the (transition to) a kinetic regime.

Toward this end we again employ the RL blast-wave ansatz to parameterize an anisotropic flow field which results in a good fit to the p_T spectra and elliptic flows of group-II particles. As in the group-I case, we decide to fix the freeze-out temperature at a value compatible with earlier blast-wave extractions, at $T_{fo} = 110$ MeV.

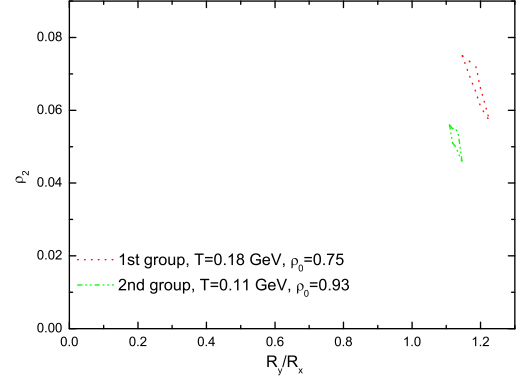


FIG. 6: (Color online) Parameter contours for ρ_2 and R_y/R_x enclosing the regions of consistency with RL blast-wave fits to p_T spectra and v_2 in the thermal regime for both freeze-out groups. The temperature, T , and average radial-flow rapidity, ρ_0 , have been fixed at $(T, \rho_0) = (180 \text{ MeV}, 0.75)$ and $(110 \text{ MeV}, 0.93)$ for group-I and -II, respectively.

Then we determine ρ_0 , ρ_2 and the eccentricity of the fireball from fits to the measured spectra and v_2 of protons and kaons for the same centrality selection of Au-Au collisions. The results are displayed in Fig. 5, corresponding to the parameter values listed in Tab. I. At kinetic freeze-out, effective chemical potentials for stable particles (pion, kaon, nucleon) are required to correctly predict the absolute normalization of their yields [33]. Neglecting chemical potentials therefore implies that we can only fit the shape of the spectra which is sufficient for our purposes here. In Boltzmann approximation, the chemical potential appears as a constant overall fugacity factor which does not affect the v_2 either. The pions are treated with Bose statistics which entails an appreciable (moderate) enhancement of the p_T spectra (v_2) at $p_T \lesssim 0.5$ GeV. At the same time, feed-down contributions are also significant in this regime. A more detailed discussion of the latter is given in App. A.

It is instructive to elaborate on the qualitative influence of the fit parameters on the observables. As is well-known from more simple blast-wave fits, the interplay of radial flow (ρ_0) and temperature (T) can be disentangled by fits to hadrons with different masses. With these 2 parameters fixed, an increase in ρ_2 leads to a rapid increase in $v_2(p_T)$ at relatively large p_T but to rather small changes at low p_T . On the contrary, increasing R_y/R_x results in a more uniform increase of $v_2(p_T)$ over a wide range of p_T . As a result, a relatively large ρ_2 , combined with a relatively small eccentricity, i.e., R_y/R_x close to unity, are favored in fitting the data. The rather tight correlation between those two parameters can be exhibited in pertinent contour plots indicating the “allowed regions” for obtaining an acceptable fit to data given their error bars, see Fig. 6. The central values of the contours for the two particle groups correspond to the values listed

in Tab. I. The contour for group-II hadrons is tighter due to the larger number of data points for bulk particles. We first note that the contours clearly exclude each other corroborating the significant evolution that the collective flow field is undergoing in the hadronic phase. More specifically, the anisotropy parameter R_y/R_x for group-II particles is smaller than for group-I, which is in line with the general expectation that the fireball becomes more spherical in the expansion. However, the flow anisotropy ρ_2 extracted from the RL blast-wave fits favors a decrease from hadronization (group-I) to kinetic decoupling of the bulk (group-II). This is contrary to the expectation from hydrodynamic expansion that $\rho_2 = (\rho_x^s - \rho_y^s)/2$ should increase if the in-plane acceleration is always larger than the out-of-plane acceleration (ρ_x^s and ρ_y^s are the surface-flow rapidities along the x - and y -direction, respectively; recall Eq. (6)). We cannot resolve this question within the present blast-wave model. A full hydrodynamic simulation could give more insight, possibly requiring substantial viscosity effects in the later stages of the hadronic evolution.

To summarize this and the previous section, we have produced a space-dependent parameterization of anisotropic flow fields which, when implemented into a rather simple thermal blast-wave description of locally equilibrated matter, provides a good overall fit to a large body of hadron data in semi-central Au-Au data in the low- p_T regime. As a key ingredient we have introduced the well established concept of sequential freeze-out including just two groups but with clearly distinct flow fields.

V. KE_T SCALING OF v_2

A signature result of ideal hydrodynamical simulations of URHICs is the mass splitting of the hadron v_2 when plotted as a function of hadron p_T , with a larger v_2 for the lighter particles at a given p_T . On the other hand, if the hydrodynamic results for the hadron v_2 are plotted versus KE_T (at a given freeze-out temperature), the splitting nearly vanishes, but not entirely. In fact, a small reverse mass ordering of v_2 is found instead, as pointed out in Refs. [13, 37]. In other words, the hydro-induced mass splitting of $v_2(p_T)$ between light and heavy particles is not large enough to render their $v_2(KE_T)$ curves degenerate. The sequential freeze-out picture advocated above may hold an explanation to this apparent discrepancy between hydrodynamic freeze-out (at fixed temperature) and experimental data (which exhibit “perfect” KE_T scaling): Random thermal motion tends to isotropize p_T distributions and thus counteracts (“dilutes”) the collective motion in producing nonzero v_2 . Thus one should expect that a gap in freeze-out temperatures between, say, (light) pions and (heavy) Ω baryons increases the mass splitting in a $v_2(p_T)$ plot (the thermal motion of pions is suppressed at lower temperatures, just enough to produce degeneracy in a $v_2(KE_T)$ representation. This

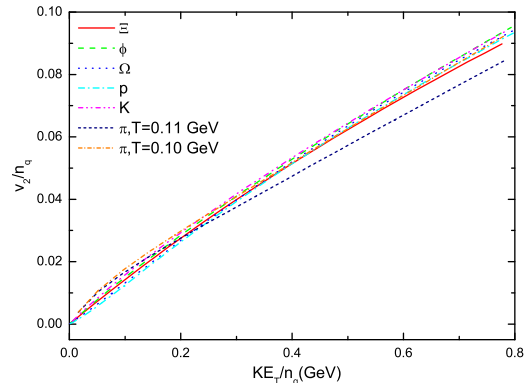


FIG. 7: (Color online) KE_T - and n_q -scaling of v_2 for different hadrons obtained within the sequential freeze-out scenario with blast-wave parameters given in Table I. The result of an slightly later freeze-out for pions at temperature 100 MeV is also shown.

appears to be a conspiracy of circumstances that leads to the empirically observed KE_T -scaling. However, the underlying mechanism (largely different hadronic rescattering cross sections) is general in the sense that it applies to different centralities, system sizes and even collision energies, presumably coupled with a rather general (local) freeze-out criterion. It therefore could be a candidate for the origin of the widely observed KE_T scaling. In the following, we quantitatively test this idea by analyzing the scaling properties within our sequential freezeout 2-source ansatz.

With the RL flow-field parameterizations and freeze-out temperatures for the two sources of group-I and group-II particles summarized in Tab. I we proceed to display the n_q -scaled hadron- v_2 as a function of the n_q -scaled hadron- KE_T in Fig. 7. We find that all the hadrons- v_2 curves follow a generic scaling very well (with slight deviations for the pions, on which we comment below), very similar to experiment. This agreement is, of course, not unexpected given that our results follow from fits to data, together with the notion that the data satisfy the scaling in the first place (or even led to its discovery). The nontrivial insight here is that our “minimalistic” approach of a sequential freeze-out scenario coupled with a rather simple parameterization of an anisotropic collective flow field, is sufficient to establish the scaling. We also recall that n_q -scaling in the equilibrated low- p_T region is not a direct consequence of quark recombination, at least not for group-II particles. To better exhibit the significance of the sequential freeze-out we compare in Fig. 8 the generic scaling curve extracted from Fig. 7 with v_2 results where the (rather heavy) Ω baryon (group-I) is frozen out from the source at $T_{fo} = 110$ MeV (as sometimes done in hydrodynamic calculations with a single freeze-out), and the (rather light) pions and kaons are frozen out from the source at $T_c = 180$ MeV (as advo-

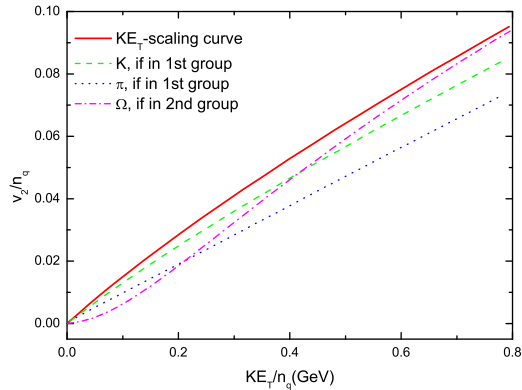


FIG. 8: (Color online) Comparison of the generic KE_T -scaling behavior of hadron v_2 extracted from Fig. 7 (thick solid line) to results for interchanging the freeze-out configurations for group-I and group-II particles. Specifically, the Ω baryon (dash-dotted line) is frozen out from the late source at $T_{fo} = 110$ MeV, while pions (dotted line) and kaons (dashed line) are frozen out from the early source at $T_c = 180$ MeV (source parameters as quoted in Tab. I).

cated in recombination models that neglect the hadronic phase). One finds a considerable breaking of both KE_T - and n_q -scaling. For the heavy particles, the increase in collective flow at the low freeze-out temperature results in an appreciable depletion of their v_2 at low KE_T (mass ordering effect), thus spoiling their compatibility with scaling. On the other hand, for pion and kaon freeze-out at higher temperature the increased thermal motion in the local rest frame dilutes the collective elliptic flow considerably and suppresses their v_2 below the scaling curve especially toward higher KE_T .

Let us return to the deviations of the pion v_2 from the scaling curve which become noticeable for $KE_T/n_q > 0.3$ GeV in Fig. 7. One may wonder whether feed-down corrections from heavier particles ($\rho \rightarrow \pi\pi$, $\omega \rightarrow 3\pi$, $\Delta \rightarrow N\pi$, etc.) could improve the situation. This question is addressed in detail in Appendix A, with the finding that the combined effect of the decay pions increases the pion v_2 at $p_T > 0.5$ GeV only a little (by a few percent). It turns out, however, that a slight decrease of the pion freeze-out temperature from 110 MeV to, e.g., 100 MeV increases the pion v_2 preferentially at higher KE_T , resulting in good agreement with the general scaling curve. In doing so we have not performed a possibly small readjustment of the flow parameters to attempt a more quantitative conclusion. The key mechanism is again a further suppression of the random thermal motion of the pions, thus augmenting the relative importance of the collective motion. A 5-10 MeV smaller freeze-out temperature is certainly compatible with experimental data, and also not unreasonable from the theoretical point of view. Pions have large resonant cross sections on all ma-

ior particle types of the bulk (pion, kaon and nucleon), and their mass being the smallest makes it plausible that their momentum spectra are frozen the latest (mass ordering of thermal relaxation times).

VI. SUMMARY AND CONCLUSIONS

In this paper we have analyzed the scaling properties of hadron elliptic flow in ultrarelativistic heavy-ion collisions, which have received considerable attention since the experimental data suggest the existence of a universal behavior possibly related to a collectively expanding partonic source. We have focused our investigations on the low- p_T regime ($p_T \lesssim 2$ GeV) where RHIC data (and hydrodynamic analysis thereof) support the assumption of a locally equilibrated medium.

In the first part of this work we have pursued the earlier idea that hadronization of the putative partonic system at RHIC proceeds through coalescence of quarks and antiquarks. Its implementation in the thermal regime requires a recombination model which obeys 4-momentum conservation and detailed balance to encode the correct equilibrium limit. The Resonance Recombination Model (RRM) satisfies these requirements. The flow field has been modeled by a blast-wave ansatz with azimuthal asymmetries which give rise to space-momentum correlations characteristic for a collectively expanding source. Using RRM we have shown that an expanding parton source converts into hadron spectra with the same collective source properties, which, to our knowledge, has not been achieved in existing models of quark coalescence. We have utilized this connection to extract quark distributions just above the critical temperature for Au-Au collisions at RHIC from measured p_T spectra and elliptic flow of multi-strange hadrons which are believed to undergo negligible final-state interactions in the hadronic phase (group-I particles).

Bulk particles with large hadronic cross sections (e.g., pion, kaons and nucleons) cannot be approximated by decoupling at the hadronization transition. We have included these particles (group-II) in our analysis by constructing another flow field at the typical kinetic freeze-out temperature of 110 MeV, and fitting the blast-wave parameters to their p_T spectra and elliptic flow. Group-II hadrons are therefore not really sensitive to quark recombination. However, we find that the sequential freeze-out picture with just two sources is well compatible with the empirically observed kinetic-energy and constituent-quark number scaling (where the latter is not directly linked to recombination). The sequential freeze-out naturally corrects for a slight breaking of KE_T scaling present in a hydrodynamic flow description for a uniform freeze-out. In particular, a smaller temperature is instrumental in suppressing the random thermal motion of the light pions and in this way bring up their v_2 toward the universal curve. In the thermal regime, CQNS of elliptic flow simply follows from the universal *linear* curve re-

sulting from KE_T scaling (i.e., it is not directly linked to recombination).

An important task of future work will be an extension of our studies to the intermediate- p_T region. Here, the onset of the kinetic regime occurs and thus off-equilibrium effects become important. While this increases the sensitivity to quark degrees of freedom, it also requires a more detailed knowledge of the reinteractions of particles, both in the QGP and hadronic phase. Initial studies using Langevin simulations for strange and heavy quarks have been reported [20], but the scaling properties found there clearly require a deeper understanding, including the effects of baryon formation and a more microscopic description of the elastic (as well as radiative) interactions in the QGP and hadronic matter.

Acknowledgments

MH acknowledges helpful discussions with H. van Hees, X. Zhao and F. Riek. This work was supported by U.S. National Science Foundation (NSF) CAREER Awards PHY-0449489 and PHY-0847538, by NSF grant PHY-0969394, by the A.-v.-Humboldt Foundation, by the RIKEN/BNL Research Center, and by DOE grant DE-AC02-98CH10886.

Appendix A: Feed-Down to Pions From Resonance Decays

Hadron-resonance decays are known to increase pion yields significantly for transverse momenta up to $p_T \simeq 0.5\text{-}1$ GeV [38]. Therefore, it is mandatory to evaluate the effect of the corresponding feed-down not only on the p_T spectra but also on the elliptic flow of the pions [39, 40]. In particular, we want to understand how feed-down affects the pion v_2 in the context of the KE_T -scaling for pion freeze-out at a temperature of $T_{fo} = 110$ MeV where some deviation from protons and kaons in group I has been identified (recall Fig. 7). The total differential pion spectrum can be decomposed as

$$\frac{dN_\pi^{\text{tot}}}{p_T dp_T d\phi_p dy} = \frac{dN_\pi^{\text{dir}}}{p_T dp_T d\phi_p dy} + \sum_R \frac{dN_{R \rightarrow \pi}}{p_T dp_T d\phi_p dy}, \quad (\text{A1})$$

where the summation is over all resonances R with significant branching fraction into final states containing pions. In our decay simulation, we include ρ , ω , K^* , Δ , η and K_0^S resonances, whose anisotropic momentum spectra, together with that of direct pions, are obtained from the RL blast-wave calculation with the same parameters as those for group II in Tab. I. The resonance decays which contribute to the final spectra occur at or after freeze-out. However, the absolute number of the feed-down contribution, which is important to determine the relative contribution to the total pion- v_2 , depends on the

chemical potentials of the resonances at kinetic freeze-out. In the interacting hadronic phase effective chemical potential need to be introduced for hadrons stable under strong interactions (pion, kaon, η , nucleon, etc.), as to conserve their total numbers which are frozen at chemical freeze-out [41–43]. Part of this procedure is to keep the strong resonances in relative chemical equilibrium, e.g., $\mu_\rho = 2\mu_\pi$ or $\mu_\Delta = \mu_N + \mu_\pi$. At RHIC, the conservation of antibaryon number is of particular importance in the overall chemistry of the hadronic phase, and thus for the actual values of the effective chemical potentials [8, 33, 44–46]. The values of the chemical potentials of the resonances at T_{fo} are quoted in the caption of Fig. 9; they are taken from Ref. [33] where they are computed from an isentropic evolution starting at chemical freeze-out at $T = 180$ MeV (consistent with our parameters for group-1 freeze-out). Note that the K_0^S decays through weak interactions but carries its own chemical potential (as does the η).

The p_T -spectra of pions from various resonance decays are compiled in Fig. 9. The decay pions generally have steeper p_T -spectra than directly produced pions, except for pions from ρ decays, similar to the observations made in Refs. [39, 40]. This is essentially a phase-space effect: pions from resonances with a small Q -value (the difference of the resonance mass and the sum over masses of its constituent quarks) tend to have a steeper p_T spectrum. The phase-space also affects the v_2 of decay pions. The momenta of pions from resonances with large Q values (like the ρ) tend to dilute the v_2 more due to the random orientation of the decay momentum, most notably at low momenta (where the decay momentum in the parent's rest frame is comparable to the parent momentum). On the other hand, pions from resonances with small Q values (like the Δ) are essentially aligned with the parent and thus preserve the elliptic flow of the parent. For those pions, the v_2 could be larger than that of the parent at the same p_T , since the momentum of the resonance is shared by several daughters. However, since the dominant source of secondary pions are ρ decays, the total pion- v_2 might not be much affected by resonance decays.

The comparison of the total pion- v_2 to the direct-pion- v_2 confirms this expectation, see Fig. 10. Therefore, feed-down contributions are not sufficient to resolve the discrepancy between the direct-pion v_2 and the generic scaling curve in the KE_T -dependence of v_2 . In comparison to previous estimates we note that in Ref. [39] a larger enhancement of the total pion- v_2 over the direct-pion v_2 was reported. In that work, the resonance decays were evaluated at T_c ; subsequent hadronic rescattering was neglected and the direct pions were computed from a quark coalescence model which does not conserve energy. Both of these approximations may be unreliable for pions at small p_T , due to their large interaction cross section and binding energy, respectively. The influence of resonance decays on pion elliptic flow was also studied in Ref. [14], where the authors assumed that direct pions follow the

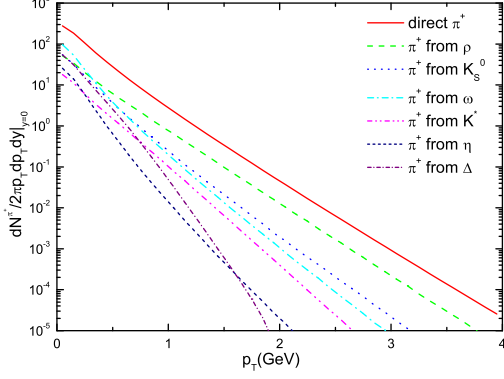


FIG. 9: (Color online) Transverse momentum spectra of pions from various resonance decays compared to direct pions (solid line) at $T_{fo} = 110$ MeV. The chemical potentials for the parent particle are resonances are $\mu_\rho = 180$ MeV, $\mu_\Delta = 460$ MeV, $\mu_{K^*} = 250$ MeV, $\mu_\omega = 270$ MeV, $\mu_\eta = 170$ MeV, resulting from a partial chemical equilibrium scenario in which chemical potentials for stable particles are $\mu_\pi = 90$ MeV, $\mu_K = 160$ MeV and $\mu_N = 370$ MeV.

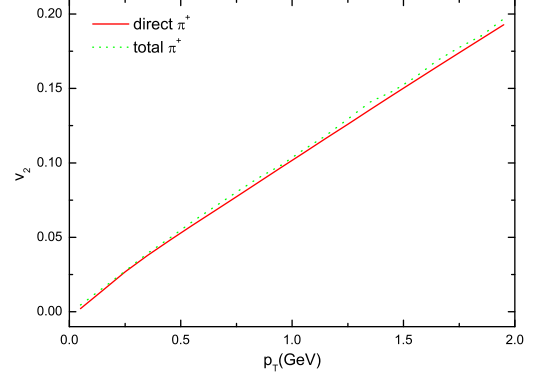


FIG. 10: (Color online) Total pion- v_2 (dashed line) compared to direct pion v_2 (solid line) at $T_{fo} = 0.11$ GeV.

KE_T -scaling and then found the scaling still holds at the 10% level when resonances are included.

-
- [1] J. Adams *et al.* (STAR Collaboration), Nucl. Phys. **A757**, 102 (2005); K. Adcox *et al.* (PHENIX Collaboration), Nucl. Phys. **A757**, 184 (2005); I. Arsene *et al.* (BRAHMS Collaboration), Nucl. Phys. **A757**, 1 (2005); B. B. Back *et al.* (PHOBOS Collaboration), Nucl. Phys. **A757**, 28 (2005).
- [2] P. Sorensen, arXiv:0905.0174v3 [nucl-ex]; S. A. Voloshin, A. M. Poskanzer, and P. Snellings, arXiv:0809.2949v2 [nucl-ex].
- [3] J. Adams *et al.* (STAR Collaboration and STAR-RHIC Collaboration), Phys. Rev. C **72**, 014904 (2005).
- [4] D. Teaney, J. Lauret, and E.V. Shuryak, Phys. Rev. Lett. **86**, 4783 (2001); D. Teaney, J. Lauret, and E.V. Shuryak, arXiv:nucl-th/0110037.
- [5] U. Heinz, arXiv:hep-ph/0407360v1; P. F. Kolb and U. Heinz, arXiv:nucl-th/0305084v2.
- [6] P. F. Kolb, J. Solfrank, and U. Heinz, Phys. Rev. C **62**, 054909 (2000).
- [7] P. Huovinen *et al.*, Phys. Lett. **B503**, 58 (2001).
- [8] T. Hirano and K. Tsuda, Phys. Rev. C **66**, 054905 (2002); T. Hirano and M. Gyulassy, Nucl. Phys. **A769**, 71 (2006).
- [9] S. A. Voloshin, Nucl. Phys. **A715**, 397c, (2003).
- [10] D. Molnar and S. A. Voloshin, Phys. Rev. Lett. **90**, 202303 (2003); R. Fries *et al.*, Phys. Rev. C **68**, 044902 (2003); V. Greco, C. M. Ko, and P. Levai, Phys. Rev. C **68**, 034904 (2003); R. Fries, V. Greco, and P. Sorensen, Ann. Rev. Nucl. Sci. **58**, 177 (2008).
- [11] S. Pratt and S. Pal, Nucl. Phys. **A749**, 268 (2005); D. Molnar, arXiv: nucl-th/0408044v2; V. Greco and C. M. Ko, arXiv: nucl-th/0505061v2.
- [12] A. Adare *et al.* (PHENIX Collaboration), Phys. Rev. Lett. **98**, 162301 (2007); B. I. Abelev *et al.* (STAR Collaboration), Phys. Rev. C **75**, 054906 (2007).
- [13] B. I. Abelev *et al.* (STAR Collaboration), Phys. Rev. C **77**, 054901 (2008).
- [14] L. A. Linden Levy *et al.*, Phys. Rev. C **78**, 044905 (2008).
- [15] R. A. Lacy and A. Taranenko, arXiv:nucl-ex/0610029v3.
- [16] J. Tian *et al.*, Phys. Rev. C **79**, 067901 (2009).
- [17] J. Jia and C. Zhang, Phys. Rev. C **75**, 031901(R) (2007).
- [18] L. Ravagli and R. Rapp, Phys. Lett. **B655**, 126 (2007).
- [19] W. Cassing and E. L. Bratkovskaya, Phys. Rev. C **78**, 034919 (2008).
- [20] L. Ravagli, H. van Hees, and R. Rapp, Phys. Rev. C **79**, 064902 (2009);
- [21] H. van Hees, V. Greco, and R. Rapp, Phys. Rev. C **73**, 034913 (2006).
- [22] O. Barannikova (for STAR collaboration), arXiv:nucl-ex/0403014.
- [23] B. Mohanty and N. Xu, J. Phys. G: Nucl. Part. Phys. **36**, 064002, (2009).
- [24] R. J. Fries *et al.*, Phys. Rev. Lett. **90**, 202303 (2003); V. Greco, C. M. Ko, and P. Levai, Phys. Rev. Lett. **90**, 202302 (2003); R. C. Hwa and C. B. Yang, Phys. Rev. C **67**, 034902 (2003).
- [25] F. Retiere and M. A. Lisa, Phys. Rev. C **70**, 044907 (2004).
- [26] J. D. Bjorken, Phys. Rev. D **27**, 140 (1983); R. C. Hwa, Phys. Rev. D **10**, 2610 (1974).
- [27] E. Schnedermann, J. Solfrank, and U. Heinz, Phys. Rev. C **48**, 2462 (1993).
- [28] R. C. Hwa and C. B. Yang, Phys. Rev. C **75**, 054904 (2007).
- [29] B. I. Abelev *et al.* (STAR Collaboration), Phys. Rev. Lett. **99**, 112301 (2007).
- [30] J. Adams *et al.* (STAR Collaboration), Phys. Rev. Lett.

- 98**, 062301 (2007).
- [31] B. I. Abelev *et al.* (STAR Collaboration), Phys. Rev. C **79**, 064903 (2009).
- [32] H. Z. Huang, J. Phys. G: Nucl. Part. Phys. **36**, 064008 (2009); J. H. Chen *et al.*, Phys. Rev. C **78**, 034907 (2008).
- [33] R. Rapp, Phys. Rev. C **66**, 017901 (2002).
- [34] R. Rapp, J. Wambach, and H. van Hees, Landolt Börnstein (Springer), New Series **I/23-A**, 4-1 (2010); arXiv:0901.3289 [hep-ph].
- [35] B. I. Abelev *et al.* (STAR Collaboration), Phys. Rev. Lett. **97**, 152301 (2006).
- [36] S. S. Adler *et al.* (PHENIX Collaboration), Phys. Rev. C **69**, 034909 (2004).
- [37] U. Heinz, arXiv:0901.4355 [nucl-th].
- [38] J. Sollfrank, P. Koch, and U. Heinz, Z. Phys. C **52**, 593 (1991).
- [39] V. Greco and C. M. Ko, Phys. Rev. C **70**, 024901 (2004).
- [40] X. Dong *et al.*, Phys. Lett. **B597**, 328 (2004).
- [41] H. Bebie *et al.*, Nucl. Phys. **B378**, 95 (1992).
- [42] C. Song and V. Koch, Phys. Rev. C **55**, 3026 (1997).
- [43] C.M. Hung and E.V. Shuryak, Phys. Rev. C **57**, 1891 (1998).
- [44] P. F. Kolb and R. Rapp, Phys. Rev. C **67**, 044903 (2003).
- [45] R. Rapp and E.V. Shuryak, Phys. Rev. Lett. **86**, 2980 (2001)
- [46] D. Teaney, arXiv:nucl-th/0204023.